

Evaluation of Nonstationarity in Annual Maximum Flood Series and the Associations with Large-scale Climate Patterns and Human Activities

Jianzhu Li · Xueyang Liu · Fulong Chen

Received: 1 September 2014 / Accepted: 7 December 2014 /
Published online: 17 December 2014
© Springer Science+Business Media Dordrecht 2014

Abstract Recent evidences of the impact of regional climate variability, coupled with the intensification of human activities, have led hydrologists to study flood regime without applying the hypothesis of stationarity. In this study, identification of nonstationarity was conducted in the form of both trend and change point in the mean of the annual maximum flood magnitudes, using Mann-Kendall and Pettitt test, respectively in Wangkuai reservoir watershed, China. The annual maximum flood series exhibited a significant decreasing trend, and the timing of change point was detected in 1979, which was consistent with the construction of large numbers of check dams and small hydraulic structures. A correlation test (Pearson correlation test) between large-scale oceanic-atmospheric patterns (El Niño Southern Oscillation (ENSO), Pacific Decadal Oscillation (PDO), North Pacific Oscillation (NPO), North Atlantic Oscillation (NAO), Atlantic Oscillation (AO)) and annual maximum flood peaks was adopted to assess the climatic causes of nonstationary flood series. It was found that NPO, NAO and AO had significant correlations with flood peak, but ENSO and PDO could not explain the variations of flood peak. In the case of human-induced nonstationarity, we proposed 2 new indices to represent the effect of human activities on flood. The new indices were proposed based on the storage capacity and drainage area of the large numbers of check dams and small hydraulic structures which were estimated with no observed data. The identification of nonstationarity for flood series and the climatic and human-induced causes could provide useful information in nonstationary flood frequency analysis.

Keywords Nonstationarity · Annual maximum flood peak · Climatic indices · Human-induced indices

J. Li (✉) · X. Liu · F. Chen
State Key Laboratory of Hydraulic Engineering Simulation and Safety, Tianjin University, Tianjin 300072,
China
e-mail: lijianzhu@tju.edu.cn

1 Introduction

Flood is a natural hazard of significant importance, resulting in both human death and economic losses in many parts of the world. In order to mitigate the losses induced by floods, many flood control works had been built on large rivers, and almost all the structures were built based on flood frequency analysis under the assumption of stationarity. However, anything in the world, including nature, human science and our knowledge, is in changing and developing. In this sense, nonstationarity exists all the time. Milly et al. (2008) had pointed out that there has been stationarity, but it is dead.

Many authors have investigated the nonstationarity in form of trends and shifts in hydrological time series at different temporal and spatial scales. The most popular trend tests include Mann-Kendall, Spearman's Rho, and linear regression (Olsen et al. 1999; Svensson et al. 2005; Shadmani et al. 2012). In many river basins, flood series exhibited a significant increasing or decreasing trend due to anthropogenic effects (Hu and Huang 2012; Gao et al. 2008; Li and Feng 2010), with many more studies than can be listed here. Although many methods for change point detection were proposed in recent years (Li et al. 2014a, 2014b), the Pettitt test was adopted in several recent studies to identify the existence of abrupt shifts in flood time series (Fritsch 2012; Villarini et al. 2009a; Villarini and Smith 2010). Despite of significant trends, the time series are not necessary to display a significant shift (change point). But most of the studies showed that there were change points for flood series accompanying with a decreasing or increasing trend (Xie et al. 2012; Wang et al. 2012), and the authors speculated that abrupt changes could be caused by both natural and anthropogenic factors such as climate patterns, changes in rainfall regimes, changes in land use and land cover and construction of engineering structures for river regulations. But Yilmaz and Perera (2013) thought increasing or decreasing behaviour of the series does not always indicate nonstationarity, and it is necessary to conduct further analysis to identify nonstationarity. They adopted three statistical tests which were augmented Dickey-Fuller, Kwiatkowski-Phillips-Schmidt-Shin, and Phillips-Perron to investigate nonstationarity in extreme rainfall time series. These three methods were commonly used in hydrological studies (Wang et al. 2005, 2006; Yoo 2007).

In the context of water resources applications, it is necessary to consider the driving causes, whether climatic and human-induced, of the observed changes in hydrological phenomena (Fritsch 2012). Olsen et al. (1999) had long recognized global climate patterns including El Niño/Southern Oscillation, the Pacific Decadal Oscillation and North Atlantic Oscillation had impact on flood nonstationarity, and they recommended to rethink the paradigm for flood frequency analysis. However, there has been relatively little attention to the role of present-day interannual climate variability. As a result, the influence of this aspect on flooding is poorly understood (IPCC 2012). Climate variability causes flood nonstationarity via the direct influence on precipitation patterns. One way is to investigate the relation to streamflows through teleconnections by statistical analysis between climatic indices and flood data (Piechota and Dracup 1999; Fritsch 2012; Casanueva et al. 2014). In addition to approaches that considered or explored changes in the observed series, process-based studies have also been conducted by incorporating simulated climate data to predict impacts of climate change on floods. Many of studies are dependent on general circulation models (GCMs) (Kwon et al. 2008; Hirabayashi et al. 2008; Alvarez et al. 2014). Gilroy and McCuen (2012) utilized a method for adjusting flood records for future nonstationary conditions based on both climate change impacts extracted from general circulation model precipitation. However, there are large uncertainties for the GCM projections.

Land use and land cover change could lead to nonstationarity in flood series as well. The removal of vegetation and soil, grading of the land surface, urbanization, and construction of drainage networks typically results in an increased magnitude and frequency of floods (Jothityangkoon et al. 2013). Forestation, soil and water conservation measures such as building check dams across rivers, and over-exploitation of groundwater caused a reduction in flood magnitude. Many authors have studied the effect of land use change on flood generation in the past decades by statistics and hydrological modeling (Farazjoo and Yazdandoost 2008; Brath et al. 2006; Saghafian et al. 2008; Li et al. 2014a, 2014b; Zeng et al. 2014). Brath et al. (2006) pointed out the sensitivity of the floods regime to land use change decreases for increasing return period of the simulated peak flow. By considering peak flows with return period ranging from 10 to 200 years, the effects of human activity seem to be noteworthy. The effects of land use changes on flood peaks depend on the nature of the flood event. Hollis (1975) underlined that the effect of the urbanization on the peak discharge is less remarkable for increasing return period of the event. Such a conclusion is justified considering that the extreme flood events are caused by storms which induce soil saturation, and therefore the reduction of the soil storativity affects the surface discharge to a smaller extent. In this regard, Niehoff et al. (2002) found that the influence of land use conditions on storm runoff generation is only relevant for convective storms with high precipitation intensities, in contrast with long lasting advective storms with low rain intensities.

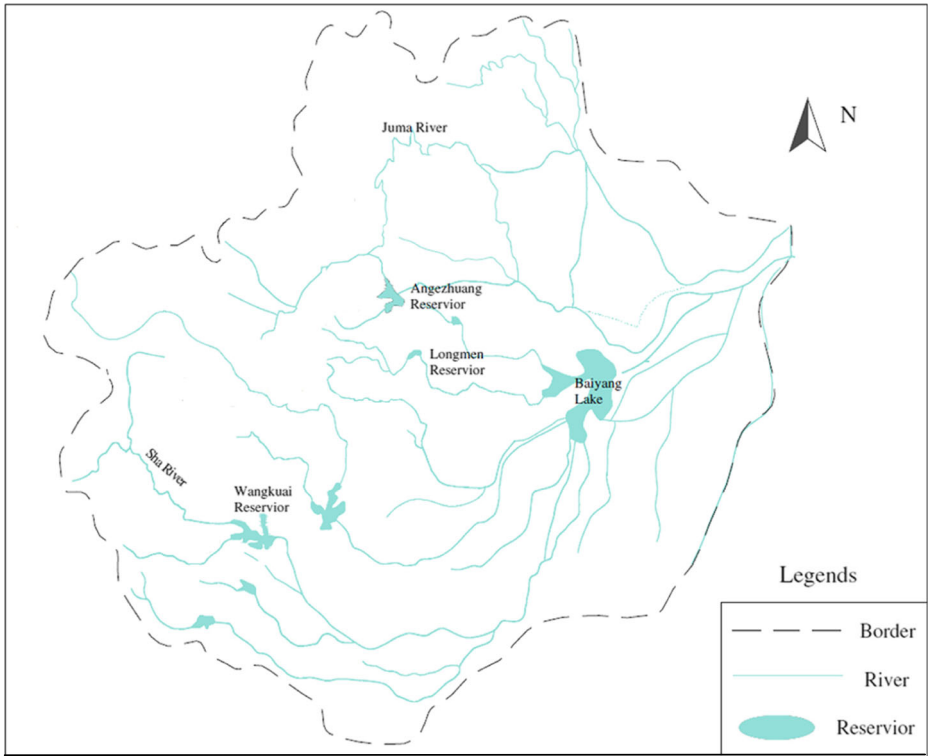
In nonstationary frequency analysis, the method that location, shape and scale parameters are expressed by covariates with linear or nonlinear forms is popular (Khaliq et al. 2006; Vasiliades et al. 2014). But the exact covariates should be associated with the hydrological variables. The aims of this study are to (1) identify the nonstationarity in annual maximum flood time series; (2) recognize the teleconnections between annual maximum flood series and climate patterns; and (3) present a human-induced index to reflect the influence of human activities on flood time series. The novelty of this paper is the human-induced index which is proposed based on the estimated total storage capacity and drainage area of the check dams and hydraulic structures with no observed data. The results of this paper could provide significant information for flood risk estimation in the river basins of environmental change.

2 Study Area

The Wangkuai reservoir located in upstream of Sha river, Daqinghe river basin (Fig. 1), which was built in June, 1958 and completed in September, 1960. The reservoir controls a drainage area of 3770 km², and the storage capacity is 13.89×10^8 m³. The reservoir was constructed for a comprehensive purpose of flood control, irrigation and electric power generation. The currently used design floods were calculated using flood data series under the assumption of stationarity.

The watershed receives an average precipitation of 600 mm, mostly in the summer (70–80 %). The annual mean temperature is 7.4 °C. The watershed is characterized by steep slopes and bedrock outcrops. Forest and grass are dominant on the hill slopes. Urban area is <2 %. Rainfall and runoff data have been monitored for a period of more than 50 years from 1956 to 2008. There are 11 rain gauges available in the study area.

Soil erosion is serious in this watershed, so soil and water conservation was carried out from 1980s, of which check dams were dominated. Small hydraulic structures and large numbers of check dams affected flood processes in this watershed. Take the area (2210 km²) controlled by Fuping station (located in the upstream of Wangkuai reservoir) as an example, there are 11 small reservoirs whose total storage capacity were up to $591.5 \times$



(a)



(b)

Fig. 1 The study area. **a** location of Wangkuai reservoir in Daqinghe river basin; **b** the Wangkuai reservoir watershed

10^4 m^3 , of which Haiyan reservoir is the largest one with storage capacity of $367 \times 10^4 \text{ m}^3$, and the design criteria is 500-year return period flood. There were also pond and retaining dams of

effective storage capacity of $148 \times 10^4 \text{ m}^3$. More than six thousand check dams were built from 1996 to 2008, but the storage capacity could not be derived by survey.

3 Data and Methods

3.1 Data

The rainstorm and flood data were provided by Hydrology and Water Resources Survey Bureau of Hebei Province. Rainfall data used in this study are measured from 11 stations and the mean rainfall was calculated by Thiessen polygon method. Water balance equation was employed to calculate inflow flood data of Wangkuai reservoir using the reservoir water level and the discharge data. The time series are from 1956 to 2008, and the data was collected on hourly basis. Several large floods were selected and analyzed in this study.

The remotely sensed land use data of 1980 and 2000 were provided by Chinese Academy of Science (Fig. 2). The land use was classified into 6 types, including forest, grassland, agricultural land, urban area, water area and unused land. The area of each land use was derived in GIS software and it was found that they kept almost invariant from 1980 to 2000.

3.2 Methods

3.2.1 Methods to Investigate Nonstationarity

Analysis was conducted to identify nonstationarity in the form of both trends and change point in the mean of the annual maximum flood magnitudes. Trends were investigated by applying the non-parametric Mann-Kendall test (Mann 1945; Kendall 1975). The non-parametric Pettitt test (Pettitt 1979) was adopted to identify the presence of change point in the mean over time.

Mann-Kendall Test The Mann-Kendall test is a non-parametric, rank-based method, and has been broadly used in trend test in streamflow, precipitation and temperature series (Burn and

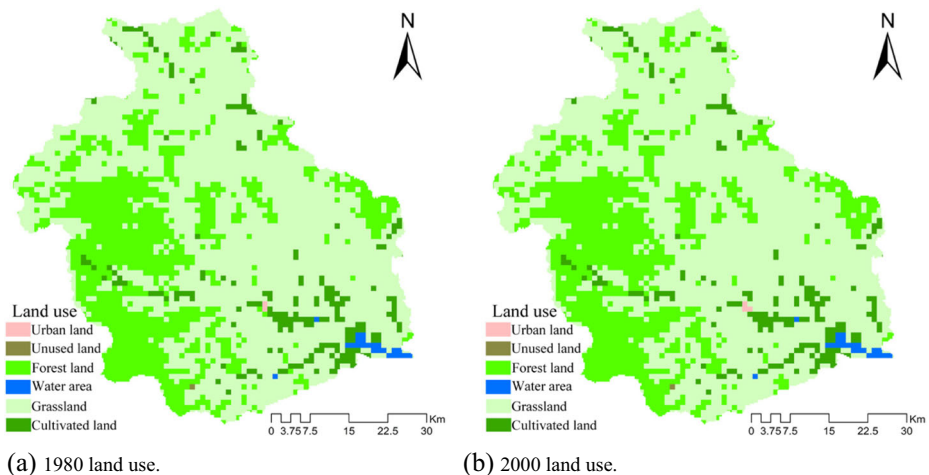


Fig. 2 Remotely sensed land use of the Wangkuai reservoir watershed

Hag 2002; Collins 2009; Fritsch 2012; Azizabadi and Khalili 2013). Given a time series of annual maximum flood peak (n years), the magnitude of the flood peak in year i is compared to each value recorded in subsequent years j ($j=i+1$ to n). For each pair of (x_i, x_j) , the sign of their difference is evaluated and the Kendall's S test statistic is calculated as:

$$S = \sum_{i=1}^{n-1} \sum_{j=i+1}^n \text{sign}(x_j - x_i) \tag{1}$$

$$\text{sign}(x_j - x_i) = \begin{cases} 1 & \text{if } x_j - x_i > 0 \\ 0 & \text{if } x_j - x_i = 0 \\ -1 & \text{if } x_j - x_i < 0 \end{cases} \tag{2}$$

The two tailed test is used. At certain probability level H_0 is rejected in favor of H_1 if the absolute value of S equals or exceeds a specified value $S_{\alpha/2}$, where $S_{\alpha/2}$ is the smallest S which has the probability less than $\alpha/2$ to appear in case of no trend. A positive (negative) value of S indicates an upward (downward) trend.

Pettitt Test The Pettitt test is a rank-based, non-parametric test, and thus does not require the data to follow a particular distribution (Pettitt 1979; Reeves et al. 2007). It considers a time series as two samples represented by x_1, \dots, x_t and x_{t+1}, \dots, x_T . For continuous data the indices $V(t)$ and $U(t)$ can be calculated from the following formula

$$U_{t,T} = U_{t-1,T} + V_{t,T} \tag{3}$$

For $t=2, \dots, T$,

$$V_{t,T} = \sum_{j=1}^T \text{sgn}(x_t - x_j) \tag{4}$$

where,

$$\text{sgn}(\theta) = \begin{cases} 1 & \theta > 0 \\ 0 & \theta = 0 \\ -1 & \theta < 0 \end{cases}$$

The most significant change point is found where the value $|U_{t,T}|$ is maximum. The approximate significance probability, $p(t)$, of a change point can then be calculated from

$$p(t) = 1 - \exp\left(\frac{-6U_{t,T}^2}{T^3 + T^2}\right) \tag{5}$$

3.2.2 Methods to Identify the Causes of Nonstationarity

Correlation Analysis A correlation test between large-scale oceanic-atmospheric patterns and annual maximum flood peaks is adopted to assess their degree of association. Three correlation tests, Pearson, Kendall and Spearman correlation test, are popular in hydrology (Niu et al. 2013; Hodgkins et al. 2003; McCormick et al. 2009), and each has its own advantages and

disadvantages. In nonstationary flood frequency analysis, linear combination of different climate indices (ENSO, PDO, et al.) is usually considered to be the external covariate. Compared with the other two methods, Pearson’s r correlation test considers the degree of linear association between two variables. So in this paper, we select Pearson correlation test to identify the correlations between climate indices and the annual maximum flood peak. Pearson’s r can be estimated as the following equation.

$$r = \frac{\sum_{i,j=1}^n (x_i - \bar{x})(y_i - \bar{y})}{\sqrt{\sum_{i=1}^n (x_i - \bar{x})^2 \sum_{j=1}^n (y_j - \bar{y})^2}} \tag{6}$$

where x_i and y_i are observations of X and Y , n is the number of observations in each series, and \bar{x} and \bar{y} are their samples averages. With using the function $corr(\cdot)$ in MATLAB, we can return a matrix of p -values for testing the hypothesis of no correlation against the alternative that there is a non-zero correlation. Each element of p -value for the corresponding element of r , if p -value is small, say less than 0.05, then the correlation r is significantly different from zero.

Index of Human-Related Nonstationarity Human-induced nonstationarity are generally caused by land use/land cover change and construction of hydraulic engineering. Land use changed almost kept invariant during 1980–2000, and the main causes of human-induced nonstationarity are the construction of large numbers of check dams for soil and water conservation in Wangkuai reservoir watershed. However, the hydrological responses had not been understood clearly in watersheds with large numbers of check dams and small hydraulic structures, because the runoff processes in the channels with check dams were difficult to simulate. Besides, observations of check dams are difficult to obtain. In China, check dams were constructed at the request of the residents without any long-term design schemes. The locations, storage capacities and outflow methods have not been inventoried and documented (Xu et al. 2013).

Lopez and Frances (2013) proposed a dimensionless reservoir index as one of the external covariates for nonstationary flood frequency analysis in continental Spanish rivers. The reservoir index was expressed by:

$$RI = \sum_{i=1}^n \left(\frac{A_i}{A_T} \right) \cdot \left(\frac{C_i}{C_T} \right) \tag{7}$$

where N is the number of reservoirs upstream of the gauge station. A_i is the catchment area of each reservoir, A_T is the catchment area of the gauge station. C_i is the total capacity of each reservoir, and C_T is the mean annual runoff at the gauge station. However, all the variables in the equation are constants in a specific period, leading to a constant RI , regardless of flood patterns. Considering the deficiency of RI , we present two new indices to reflect the influences of check dams on flood peak and volume, respectively. They are expressed as:

$$CDI_p = \frac{\Delta FP_i}{FP_i} \tag{8}$$

$$CDI_v = \frac{\Delta FV_i}{FV_i} \tag{9}$$

where, CDI_p and CDI_v are indices for flood peak and volume influenced by check dams and small hydraulic structures, respectively. ΔFP_i and ΔFV_i are the decreased flood peak and flood volume for the annual maximum flood peak and volume for the flood in the i th year, respectively, caused by construction of check dams and small hydraulic structures. FP_i and FV_i are the annual maximum flood peak and volume for the flood in the i th year under pre-1979 land use conditions, respectively.

In order to analyze the effects of upstream check dams and small hydraulic structures on flood peak and flood volume of the Wangkuai reservoir, their total storage capacity and drainage area should be estimated. Because of the large numbers of check dams, the storage capacity could not be obtained by survey directly, and historical observed rainstorm and flood data must be used. Two similar heavy rainstorms (similar total rainfall depth, intensity, duration and spatial distribution) were selected, which should generate similar flood processes, and the surface runoff could fill up the small reservoirs and check dams upstream. Compared with the two flood processes, the difference between the surface runoff of the two flood events is the total storage capacity of the small reservoirs and check dams upstream.

The rainstorm and flood data during undisturbed period were selected, and the relationship between rainfall intensity and flood peak was established, and an equation could be fitted. And then several rainfall events during the disturbed period whose rainfall peak occurred in the beginning were selected, and the theoretical flood peak Q_t could be calculated using the fitted equation. The decreased flood peak due to small reservoirs and check dams is the difference between the theoretical flood peak Q_t and observed flood peak Q_o , and there will be Eq. (4) as follows:

$$\frac{A_r}{A} = \frac{Q_t - Q_o}{Q_t} \quad (10)$$

where A_r is the drainage area of upstream small reservoirs and check dams, and A is the area controlled by the Wangkuai reservoir. So we can get A_r by Eq. (10).

Since the beginning of construction of check dams was in approximately 1980, we divided the entire period into 2 sub-periods, i.e. before and after 1980 to calculate ΔFP_i and ΔFV_i . For each annual maximum flood process before 1980, the surface discharge should be decreased by the proportion A_r/A till all the upstream reservoirs and check dams reach their storage capacity if the surface discharge generated in A_r area is greater than the storage capacity. If the flood is relatively small that the surface discharge generated in A_r area is less than the storage capacity, the surface runoff hydrograph should decreased by the proportion A_r/A from beginning to the end. In contrast, for each annual maximum flood process after 1980, the surface discharge should be increased by the proportion A_r/A . Then each flood process under the land conditions before and after 1980 could be derived and ΔFP_i and ΔFV_i were the difference between the same flood process under the land conditions before and after 1980. Thus, the calculated CDI_p and CDI_v are different for each flood.

4 Results

4.1 Identification of Nonstationarity for Annual Maximum Flood

4.1.1 Trends in Annual Maximum Flood Peak Series

The annual maximum flood peaks against time were plotted in Fig. 3. A downward trend can be seen for the entire time series, because large floods occurred in years of 1956, 1959 and

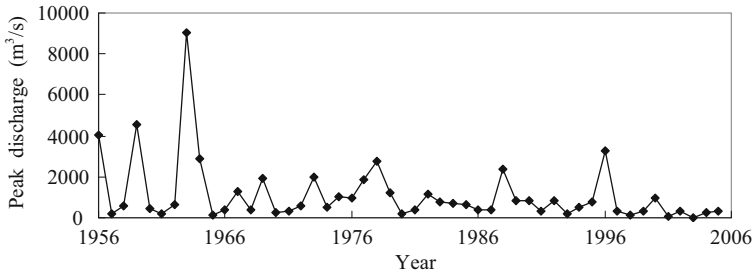


Fig. 3 Annual maximum peak discharge of Wangkuai reservoir

1963, i.e. the initial period of the time series. If the 3 peaks were excluded, no visible trend could be detected.

So the Mann-Kendall trend test was conducted at significance level of 5 %. The value of S was -2.4 , exceeding the value $S_{\alpha/2}(-1.96)$. Thus, the null hypothesis of no trend was rejected, with a decreasing trend identified.

4.1.2 Change Point in Annual Maximum Flood

The Pettitt test was performed to investigate the presence of a statistically significant shift in the mean of the annual maximum flood series at 10 % significant level. Figure 4 shows the change point of the annual maximum peak discharge time series. The possible change points are 1979 and 1996. As can be seen in Fig. 3, it was a very large flood event for 1996 maximum flood, the floods before and after 1996 were relatively small, so 1996 could not be considered as a change point. Therefore, the occurrence of change point in annual maximum peak discharge was 1979.

Based on the results of change point detection, peak flood series could be divided into two sub-series which were preceding and following the change point, namely 1956–1979 and 1980–2005. Compared with the means of the two sub-series, the annual maximum peak discharge was 58.3 % lower during 1980–2005 than that in 1956–1979, which was a relatively large percent. But compared with the rainfall amounts corresponding to the peak floods, there was just 33.2 % lower for the period of 1980–2005 than 1956–1979. Land use and land cover must cause flood peak decrease as well. Some of the small reservoirs were built on the upstream of Wangkuai reservoir, and listed in Table 1. Most of them were completed during the period 1970–1980, especially the largest one, Haiyan reservoir, which has the storage

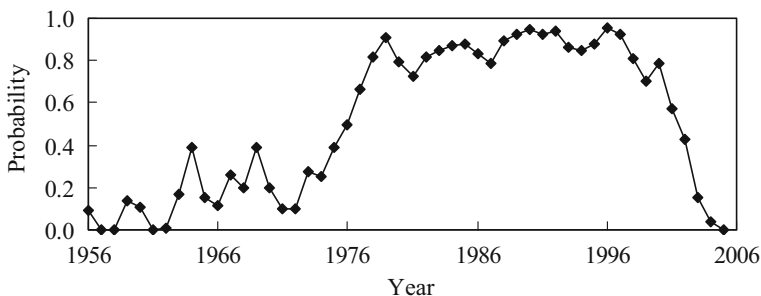


Fig. 4 Pettitt test results of the annual maximum peak discharge

Table 1 The main small reservoirs on the upstream of Wangkuai reservoir

Small reservoir	Storage capacity (10^4 m^3)	Year of being built	Drainage area (km^2)
Haiyan	367.0	1979	12.3
Mapeng	45.0	1996	52.0
Tagou	10.0	1978	5.5
Dahewan	4.0	1981	33.1
Duizigou	14.0	1975	1.2
Shijia	22.0	1973	9.8
Waquangou	12.0	1974	1.8
Yujiatai	10.2	1975	5.7

capacity much larger than the total of the others was completed in 1979. Besides, large numbers of check dams were constructed during that period for soil and water conservation. These small reservoirs and large numbers of check dams were consistent with the timing of occurrence of change point.

4.2 The Causes of Nonstationarity for Annual Maximum Flood

4.2.1 Climatic Causes of Nonstationarity

Large-scale oceanic-atmospheric patterns were investigated as possible sources of the nonstationarity in annual maximum flood series. Correlation analysis was made to identify the relation between annual maximum flood peak and climatic indices. Five large-scale oceanic-atmospheric patterns (Pacific Decadal Oscillation (PDO), North Pacific Oscillation (NPO), North Atlantic Oscillation (NAO), Atlantic Oscillation (AO) and El Niño/Southern Oscillation (ENSO)) were chosen to check their Teleconnections with annual maximum flood series. NINO3 is used herein to describe ENSO.

The time series employed in the correlation test were obtained according to Salvadori (2013). For each climate pattern, the climate index in different lead time (3, 6 and 9 months) was made correlation analysis with annual maximum flood peak. The recorded annual maximum flood peak discharges Q_{\max} , but not the natural logarithm form ($\ln Q_{\max}$) as other authors adopted (Ward et al. 2014), were used to analyze the correlation with climate indices.

Pearson correlation test was performed at 5 % significance level to assess the degree of association between annual maximum flood peak series and the climate indices series for a given lead time. Table 2 shows the results of correlation analysis for each combination of

Table 2 Results of Pearson correlation analysis

Climatic indices	3 months		6 months		9 months	
	r	p -values	r	p -values	r	p -values
PDO	-0.2141	0.1397	-0.1518	0.2976	-0.1385	0.3425
NINO3	-0.1736	0.2329	-0.0271	0.8536	-0.0570	0.6974
NPO	0.2584	0.0730	0.2813	0.0500	-0.1370	0.3481
AO	0.1300	0.3733	0.0172	0.9065	-0.3556	0.0121
NAO	0.1563	0.2836	-0.1118	0.4444	-0.4408	0.0015

climate index and lead time. The greatest positive teleconnections with maximum annual flood peaks was observed for NPO with 6-months lead time at 5 % significance level, and AO and NAO exhibited negative teleconnections with maximum annual flood peaks with 9-months lead time. No teleconnections were found for both PDO and NINO3 with maximum annual flood peaks with any lead time. The teleconnections of annual maximum peak discharge with ENSO exhibited different results in different regions. Ward et al. (2014) found ENSO exerted a significant influence on annual floods in river basins covering over a third of the world’s land surface. Olsen et al. (1999) examined climate variability and flood frequency for the upper Mississippi and lower Missouri rivers, and ENSO, PDO, NAO explained very little of the variations in flow peaks. However, significant correlation with flood events justifies the use of climate indices as external covariates in flood frequency analysis in several studies (El Aldouni et al. 2007; Ouarda and El Aldouni 2011).

4.2.2 Nonstationarity Caused by Check Dams

Estimation of Total Storage Capacity of the Upstream Small Reservoirs and Check Dams The flood events occurred on August 12, 1964 and August 5, 1996 were selected to estimate the total storage capacity of the upstream small reservoirs and check dams. The August 12, 1964 rainfall events had a total rainfall amount of 132.4 mm with the maximum hourly rainfall intensity 10.8 mm/h, and the duration was 29 h. While the August 5, 1996 rainfall event had a total rainfall amount of 134.8 mm with the maximum rainfall intensity 7.9 mm/h, and the duration was 30 h. The other characteristics of the two rainfall events were listed in Table 3. We can see the characteristics of the two rainfall events are similar. The former rainfall event generated 39.19 mm surface runoff, while the latter generated 35.24 mm surface runoff, and the difference 3.95 mm is considered to be stored by the small reservoirs and check dams upstream. Since the large rainfall amount of the selected events, the small reservoirs and check dams were assumed to reach their storage capacities, and 3.95 mm is the total storage capacity of the upstream hydraulic structures (Table 4).

Assessment of the Drainage Area of the Upstream Small Reservoirs and Check Dams We selected 8 flood events during the undisturbed period (1956–1979) (Table 3) to establish the rainfall intensity-flood peak relationship. And we found that flood peak occurred approximately 3 or 4 h later than the maximum 3 h maximum rainfall. An exponential function was fitted for the data as Eq. (11), and the correlation coefficient R^2 was 0.8254 as in Fig. 5.

$$Q_t = 74.679\exp(0.1179P_3) \tag{11}$$

Where Q_t is the discharge in m^3/s , P_3 is the maximum 3 h rainfall amount in mm.

Then we selected 4 flood events during the disturbed period to estimate the drainage area of the upstream small reservoirs and check dams (Table 5). The calculated flood discharge based on Eq. (11) was compared with the discharge 3 h after the maximum 3 h rainfall, and A_t/A

Table 3 The characteristics of the selected rainfall events

Rainfall events	Rainfall amount (mm)	Duration (h)	Maximum rainfall intensity (mm)	Antecedent rainfall (mm)
August 12, 1964	132.4	29	10.8	76.2
August 5, 1996	134.8	30	7.9	75.8

Table 4 The selected flood events during undisturbed period

Flood events	Maximum 3 h rainfall intensity(mm)	Flood peak(m ³ /s)
July 10, 1958	16.1	587.00
July 24, 1962	13.3	655.6
August 7, 1963	37.2	9036.4
August 12, 1964	30.3	2875.5
August 16, 1966	18.8	342.2
August 4, 1967	21.2	1296.5
June 25, 1971	16.4	341.0
August 14, 1973	32.0	1987.9

could be estimated by Eq. (10). The A_r/A values were different for each selected flood event, but the difference was small, and we chose the mean, 34.6 %, as the A_r/A value. So the drainage area of the upstream small reservoirs and check dams was 1304 km².

Based on the storage capacity and drainage area, the CDI_p and CDI_v were calculated for each flood, and they were shown in Fig. 6. Different from the RI index proposed by Lopez and Frances (2013), the CDI_p and CDI_v varied each year for different flood magnitudes. Generally, the values of CDI_p and CDI_v for large floods in 1956, 1963 and 1996 were small, because of the relatively large flood volumes in comparison with the storage capacity of the upstream check dams. In case of small floods which were dominated by subsurface flow, the values of CDI_p and CDI_v were small as well, because a small part of surface flow could be stored upstream. The value of CDI_p for 1963 flood event was 0, because the large amount of surface runoff before flood peak could fill up the upstream small check dams and reservoirs, and had no effect on the peak discharge.

5 Discussion and Conclusions

It was assumed that annual maximum flood series were stationary in traditional methods for hydraulic structure design and flood risk forecasting, implying a constant flood risk associated with a given flow magnitude. however, the effects of climate variability/change can not be neglected, and in some severely impaired watersheds

Fig. 5 The relationship between rainfall intensity and flood peak

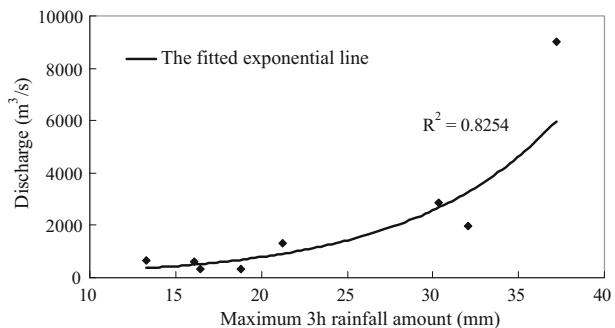


Table 5 The selected flood events during disturbed period and the estimated A_r/A

Flood events	Maximum 3 h rainfall(mm)	Observed discharge(m ³ /s)	Calculated discharge(m ³ /s)	$A_r/A(\%)$
July 22, 1989	20.3	553.0	820.1	32.6
August 26, 1990	23.3	858.7	1267.0	32.2
July 8, 1994	19.8	497.2	773.7	35.7
August 18, 1999	15.5	291.8	468.9	37.8
Mean				34.6

human activities are critical factors affecting annual maximum floods. This paper identified the nonstationarity in annual maximum flood peak series by trend and change point test for the Wangkuai reservoir watershed, Daqinghe river basin, China. At the 5 % significance level, decreasing trend was detected, and a statistically significant change point in 1979 was identified at the 10 % significance level, which provided further evidence “stationarity is dead” (Milly et al. 2008).

Teleconnections of large scale ocean–atmosphere patterns were investigated as potential climatic source of nonstationarity in annual maximum flood series. For NPO, statistically significant relationship was observed with 6-months lead time, and for AO and NAO, significant relationships were observed with 9-months lead time. But no statistically significant relationships were found for PDO and NINO3. Since the relatively short flood series from 1956 to 2005, we did not use a 10-year window to smooth the series as used by Salvadori (2013).

The small reservoirs on the upstream of Wangkuai reservoir coincided with the change point in 1979 for annual maximum flood series. However, large numbers of check dams were constructed after 1970, and no available data for these check dams. Therefore, the storage capacity of the check dams and small reservoirs upstream was estimated by two similar large flood events occurred in undisturbed and disturbed periods, respectively. The estimated storage capacity was 3.95 mm, equals to 1489 million m³, larger than the total storage capacity (739 million cubic meters) of the small reservoirs. Because there are large numbers of check dams, the estimated total storage capacity (1489 million m³) was considered reasonable. The drainage area of the small reservoirs was 460 km², and the estimated drainage area (1304 km²) of the small hydraulic structures including the small reservoirs was larger, so the result was considered reasonable as well. Although there were large numbers of check dams, we presented a feasible method to estimate their storage capacity and drainage area. Based on the assessed storage capacity and drainage area, human-induced indices, CDI_p and CDI_v , were

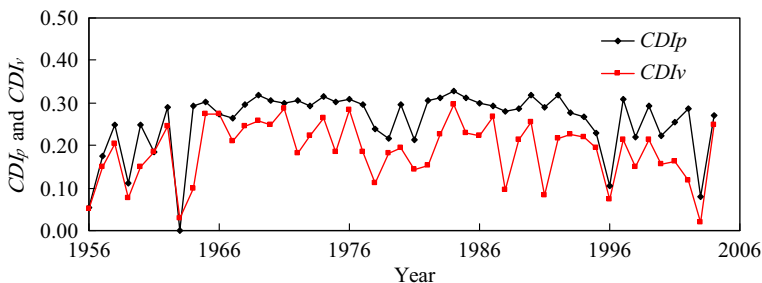


Fig. 6 Check dams and small reservoir indices in Wangkuai reservoir watershed

proposed which varied depending on the flood patterns. The new human-induced indices were presented on the basis of *RI* proposed by Lopez and Frances (2013), but seemed more reasonable. However, these two indices were formed under the condition that land use and land cover kept invariant, and check dams and small reservoirs were dominant in the watershed.

In watersheds where both land use/land cover change and large numbers of check dams were dominant, new methods should be developed to estimate the storage capacity and drainage area, and land use/land cover should be included as a control factor on flood series. One example is the study made by Villarini et al. (2009b) who incorporated a population index to describe the impact of land use changes in an urban watershed.

Future works should be focused on accounting for both natural and anthropogenic factors in flood frequency analysis, especially using the human-induced indices proposed in this paper and the large scale climate patterns. However, how to combine the two factors in a comprehensive model is still not clear and it represents a major challenge for the scientific community. Lopez and Frances (2013) provided an effective way, but at present there are no long-term predictions for such climate indices as PDO, ANO, AO, and human-induced indices.

Acknowledgments This work was supported by National Natural Science Foundation of China (No. 51209157). We are also grateful to Hydrology and Water Resource Survey Bureau of Hebei Province for providing the hydrometeorological data.

References

- Alvarez UFH, Trudel M, Leconte R (2014) Impacts and adaptation to climate change using a reservoir management tool to a northern watershed: application to Lievre river watershed, Quebec, Canada. *Water Resour Manag* 28:3667–3680
- Azizabadi M, Khalili D (2013) Seasonality characteristics and spatio-temporal trends of 7-day low flows in a large, semi-arid watershed. *Water Resour Manag* 27:4897–4911
- Brath A, Montanari A, Moretti G (2006) Assessing the effect on flood frequency of land use change via hydrological simulation (with uncertainty). *J Hydrol* 324:141–153
- Burn DH, Hag EMA (2002) Detection of hydrologic trends and variability. *J Hydrol* 255:107–122
- Casanueva A, Puebla CR, Frias MD et al (2014) Variability of extreme precipitation over Europe and its relationships with teleconnection patterns. *Hydrol Earth Syst Sci* 18:709–725
- Collins MJ (2009) Evidence for changing flood risk in New England since the late 20th century. *J Am Water Resour Assoc* 45:279–290
- El Aldouni S, Ouarda T, Zhang X et al (2007) Generalized maximum likelihood estimators for the nonstationary generalized extreme value model. *Water Resour Res* 43:1–13
- Farajzoo BSH, Yazdandoost BBF (2008) Flood intensification due to changes in land use. *Water Resour Manag* 22:1051–1067
- Fritsch CE (2012) Evaluation of flood risk in response to climate variability. Dissertation, Michigan Technological University
- Gao Q, Huo L, Gong JX (2008) Trend analysis on flooding changes in Urumqi river. *Desert and Oasis Meteorol* 2:30–33
- Gilroy KL, McCuen RH (2012) A nonstationary flood frequency analysis method to adjust for future climate change and urbanization. *J Hydrol* 414:40–48
- Hirabayashi Y, Knäe S, Emori S et al (2008) Global projections of changing risks of floods and droughts in a changing climate. *Hydrol Sci J* 53:754–772
- Hodgkins G, Dudley R, Huntington T (2003) Changes in the timing of high river flows in New England over the 20th century. *J Hydrol* 278:244–252
- Hollis GE (1975) The effect of urbanization on flood of different recurrence interval. *Water Resour Res* 11:431–435

- Hu HY, Huang GR (2012) Variation trends of rainfall and flood in Dongtiaoxi basin. *Water Power* 38:14–17
- IPCC (2012) Managing the risks of extreme events and disasters to advance climate change adaptation. A special report of working groups I and II of the Intergovernmental Panel on Climate Change. Cambridge University Press, Cambridge
- Jothityangkoon C, Hirunteeayakul C, Boonrawd K et al (2013) Assessing the impact of climate and land use changes on extreme floods in a large tropical catchment. *J Hydrol* 190:88–105
- Kendall M (1975) Rank correlation measures. Charles Griffin, London
- Khaliq MN, Ouarda TBMJ, Ondo JC et al (2006) Frequency analysis of a sequence of dependent and/or non-stationary hydro-meteorological observations: A review. *J Hydrol* 329:534–552
- Kwon HH, Brown C, Lall U (2008) Climate informed flood frequency analysis and prediction in Montana using hierarchical Bayesian modeling. *Geophys Res Lett* 35, L050404
- Li JZ, Feng P (2010) Effects of precipitation on flood variations in the Daqinghe river basin. *J Hydraul Eng* 41: 595–600
- Li JZ, Feng P, Chen FL (2014a) Effects of land use change on flood characteristics in mountainous area of Daqinghe watershed, China. *Nat Hazards* 70:593–607
- Li JZ, Tan SM, Wei ZZ et al (2014b) A new method of change point detection using variable fuzzy sets under environmental change. *Water Resour Manag* 28:5125–5138
- Lopez J, Frances F (2013) Non-stationary flood frequency analysis in continental Spanish rivers, using climate and reservoir indices as external covariates. *Hydrol Earth Syst Sci* 17:3189–3203
- Mann HB (1945) Nonparametric tests against trend. *Econometrica* 13:245–259
- McCormick BC, Eshleman KN, Griffith JL et al (2009) Detection of flooding responses at the river basin scale enhanced by land use change. *Water Resour Res.* doi:10.1029/2008WR007594
- Milly PCD, Betancourt J, Falkenmark M et al (2008) Stationarity is dead: Whither water management? *Science* 319:573–574
- Niehoff D, Fritsch U, Bronstert A (2002) Land-use impacts on storm runoff generation: scenarios of land-use change and simulation of hydrological response in a meso-scale catchment in SW-Germany. *J Hydrol* 267: 80–93
- Niu J, Chen J, Sivakumar B (2013) Teleconnection analysis of runoff and soil moisture over the Pearl river basin in South China. *Hydrol Earth Syst Sci Discuss* 10:11943–11982
- Olsen JR, Stedinger JR, Matalas NC et al (1999) Climate variability and flood frequency estimation for the Upper Mississippi and Lower Missouri rivers. *J Am Water Resour Assoc* 35:1509–1523
- Ouarda T, El Aldouni S (2011) Bayesian nonstationarity frequency analysis of hydrological variables. *J Am Water Resour Assoc* 47:496–505
- Pettitt A (1979) A non-parametric approach to the change-point problem. *Appl Stat* 28:126–135
- Piechota TC, Dracup JA (1999) Long-range streamflow forecasting using El Niño-Southern Oscillation indicators. *J Hydrol Eng* 4:144–151
- Reeves J, Chen J, Wang XL et al (2007) A review and comparison of change point detection techniques for climate data. *J Appl Meteorol Climatol* 46:900–915
- Saghafian B, Farazjoo H, Bozorgy B et al (2008) Flood intensification due to changes in land use. *Water Resour Manag* 22:1051–1067
- Salvadori N (2013) Evaluation of non-stationarity in annual maximum flood series of moderately impaired watersheds in the upper Midwest and Northeastern United States. Dissertation, Michigan Technological University
- Shadmani M, Marofi S, Roknian M (2012) Trend analysis in reference evapotranspiration using Mann-Kendall and Spearman's Rho tests in arid regions of Iran. *Water Resour Manag* 26:211–224
- Svensson C, Kundzewicz WZ, Maurer T (2005) Trend detection in river flow series: 2. Flood and low-flow index series. *Hydrolog Sci J* 50:811–824
- Vasiliades L, Galiatsatou P, Loukas A (2014) Nonstationary frequency analysis of annual maximum rainfall using climate covariates. *Water Resour Manag.* doi:10.1007/s11269-014-0761-5
- Villarini G, Serinaldi F, Smith JA et al (2009a) On the stationarity of annual flood peaks in the continental United States during the 20th century. *Water Resour Res.* doi:10.1029/2008WR007645
- Villarini G, Smith JA (2010) Flood peak distributions for the eastern United States. *Water Resour Res.* doi:10.1029/2009WR008395
- Villarini G, Smith JA, Serinaldi F et al (2009b) Flood frequency analysis for nonstationary annual peak records in an urban drainage basin. *Adv Water Resour* 32:1255–1266
- Wang C, Zhou XP, Wang WS (2012) Comprehensive diagnosis of change point of flood series in Kuye river. *Water Resour Power* 30:50–53
- Wang W, Van Gelder PHAJM, Vrijling JK (2005) Trend and stationarity analysis for streamflow processes of rivers in Western Europe in the 20th century. IWA International Conference on water economics, statistics, and finance, Rethymno, Greece, 8–10 July 2005.

- Wang W, Vrijling JK, Van Gelder PHAJM et al (2006) Testing for nonlinearity of streamflow processes at different timescales. *J Hydrol* 322:247–268
- Ward PJ, Eisner S, Florke M et al (2014) Annual flood sensitivities to El Niño-Southern Oscillation at global scale. *Hydro Earth Syst Sci* 18:47–66
- Xie JH, Xie P, Xu B et al (2012) Analysis of multi-scale flood series alteration in the East river basin. *J Water Resour Res* 1:370–374
- Xu YD, Fu BJ, He CS (2013) Assessing the hydrological effect of the check dams in the Loess Plateau, China, by model simulations. *Hydrol Earth Syst Sci* 17:2185–2193
- Yilmaz AG, Perera BJC (2013) Extreme rainfall non-stationarity investigation and intensity-frequency-duration relationship. *J Hydrol Eng*. doi:10.1061/(ASCE)HE.1943-5584.0000878
- Yoo SH (2007) Urban water consumption and regional economic growth: the case of Taejeon, Korea. *Water Resour Manag* 21:1353–1361
- Zeng H, Feng P, Li X (2014) Reservoir flood routing considering the non-stationarity of flood series in North China. *Water Resour Manag* 28:4273–4287